Title: Proving Osteoinductive Potential of a Decellularized Xenograft Bone Substitute

Running Title: Osteoinductivity in a Porcine Xenograft

BASIC RESEARCH ARTICLES

Abstract

Background: Large bone defects remain a major clinical challenge for orthopaedic surgeons. Tissue engineered bone grafts have garnered increased attention as a solution to this problem. One ideal property of any bone graft is osteoinductivity or the ability to stimulate progenitor cell differentiation into a bone forming lineage.

Questions:

a. Is the osteoinductive potential of a porcine bone xenograft maintained *in vitro* after undergoing a novel decellularization and oxidation process?
b. Are porcine bone scaffolds osteoinductive in an *in vivo* animal model?

Methods:

a. *In Vitro* – C2C12 pre-osteoblasts were seeded on the scaffold or a commercial grade demineralized bone matrix (DBM) to study osteogenic differentiation and compare osteoinductive potential. MC3T3-E1 pre-osteoblasts were seeded on the scaffold and compared to a control monolayer to identify early markers of osteogenic differentiation.
b. *In Vivo* – MC3T3-E1-seeded scaffolds were implanted subcutaneously in mice and assessed for markers of early osteogenic differentiation, new bone formation (micro-computed tomography and histological assessment), and vascular infiltration (histology).

Results:

Osteoinductive potential was demonstrated in *in vitro* experiments by similar osteogenic marker expression compared to DBM and significantly greater expression than a control monolayer.

Osteoinductivity was confirmed with *in vivo* experiments showing both new bone formation and vascular infiltration.

Conclusion:

Porcine bone maintains osteoinductive properties after decellularization and oxidation.

Clinical Relevance:

This construct could potentially serve as a bone graft substitute maintaining the osteoinductive potential of native bone. The unrestricted supply and controlled donor biology may satisfy a large clinical need for orthopaedic cases requiring bone grafting.

Introduction

Management of large bone defects resulting from trauma, infection, or tumor resection remains a major clinical challenge for orthopaedic surgeons[1-3]. These defects are considered critical bone defects if they are unlikely to heal spontaneously during a patient's lifetime and are typically larger than twice the width of the diaphysis[4]. The gold standard for treatment is the use of autologous bone graft; however, due to the associated morbidity and lack of adequate bone stock or donor sites, alternative grafts are commonly used. The ideal bone graft is osteoconductive, osteogenic, and osteoinductive[1]. Osteoconductivity is the ability for the bone graft to allow osseous growth on the surface, or within its pores[5]. Osteogenic grafts retain living bone cells[5]. Osteoinductivity is the ability to stimulate progenitor cells to differentiate into a bone forming cell lineage[5,6].

Alternative bone grafts include allografts and tissue engineered bone substitutes[1,4]. Allograft use risks disease transmission and has limited availability from young, healthy donors[7,8]. Tissue engineered constructs include synthetics and xenograft-derived alternatives[4]. The advantage of synthetic bone replacements is that the constructs can be manufactured to custom structure[9]. Furthermore, osteogenicity can be artificially re-created by pre-seeding osteogenic cells onto the material prior to implantation. Osteoinductivity, however, requires the construct be able to induce cell differentiation, and therefore is more difficult to re-create[6,10,11]. Xenografts are one potential way to utilize the natural osteoinductive properties of native bone without using an allograft. Swine may be the ideal species for xenotransplantation due to physiologic compatibility with humans[12,13]. However; porcine xenotransplantation is potentially dangerous due to the presence of the alpha-gal epitope which can induce a severe inflammatory response in

61 human hosts[14,15]. Our laboratory developed a novel decellularization process that
62 successfully renders porcine soft tissues sterile and removes the alpha-gal epitope[16-19].
63 We have applied this process to porcine cancellous bone and demonstrated that the
64 construct was successfully decellularized and maintained native structural properties,
65 therefore preserving the construct's osteoconductivity[19,20]. Proteomics data also showed
66 that important growth factors believed to have a critical role in cell differentiation and
67 osteoinductivity were also preserved on the scaffold. However, the clinical relevance and
68 biologic function of these proteins after chemical processing are unknown.

69 Therefore, the current research project aimed to:

70 **1)** Demonstrate osteoinductive potential of a porcine xenograft-derived bone
71 scaffold *in vitro*.
72 **2)** Prove the osteoinductive potential is maintained in an *in vivo* model.

73 **Materials and Methods**

74 *In vitro* and *in vivo* experiments were designed to determine if a novel
75 decellularization and oxidation protocol applied to porcine bone resulted in an
76 osteoinductive bone scaffold. Scaffolds were processed using methods previously
77 described[17]. Briefly, cancellous bone was harvested from the distal metaphysis of
78 porcine femurs collected from an abattoir and subjected to a chemical decellularization
79 and oxidation protocol using combinations of deionized water, trypsin, antimicrobials,
80 peracetic acid, and triton X-100. Residual peracetic acid was cleared from specimens by
81 serial water washes until PAA levels were below the limits of detection (0.5 parts per
82 million) with high sensitivity PAA test strips (Quantofix® peroxides test sticks, Sigma).

Scaffolds were lyophilized and frozen at -80°C until further use. Previous proteomics experiments by our group have demonstrated that following this process the protein composition of the scaffold is similar to that of a commercial DBM product[19] Mass spectrometry demonstrated that in addition to the expected abundance of structural proteins, such as collagen alpha-1 and -2 chains, there were also notable similarities in the growth factors preserved on the scaffold and commercial DBM samples analyzed. Proteins such as chondroadherin, lumican, fibromodulin and biglycan play critical roles in cell differentiation, intra-cellular cascade signaling, and extra-cellular matrix assembly, and were found on both the porcine scaffold and human DBM.

Two different cell lines were chosen for indirect quantification of the scaffold's osteoinductive potential. C2C12 (ATCC® CRL1772™, Rockville, MD) is a mouse myoblast cell line that differentiates into osteoblasts in the presence of bone morphogenetic protein (BMP)-2 and is commonly used in osteoinduction studies[21-25]. MC3T3-E1 subclone 4 cells (ATCC® CRL2593™) were chosen as a second cell line for testing of the scaffold's osteoinductive potential. These cells are an osteoblast precursor derived from C57BL/6 mice and previously used to study osteoinductive potential[26,27].

In Vitro

Scaffolds or cancellous DBM sheets (Musculoskeletal Transplant Foundation, Edison NJ) (n=77 per group) were seeded with $1x10^6$ C2C12 cells. As a negative control, cells were also seeded onto gelfoam sponges (Cardinal Health) which have very limited biologic activity. The C2C12 cell line was passaged in DMEM supplemented with penicillin/streptomycin and 10% FBS, never exceeding 80% confluence in order to avoid terminal differentiation and myoblastic depletion. Cells were harvested at passage 4 and

106 suspended in 100 µL aliquots before being seeded onto constructs. Constructs were moved
107 into Petri dishes covered with media and incubated for 24 hours to allow cell attachment
108 to the matrix.. After 24 hours of incubation Samples from each group (n=11) were taken
109 for analysis while the remaining were separated for continued incubation in 2 different
110 medias: 1) Osteogenic Media (OM)[28-31] consisting of DMEM with 10 mM β-
111 Glycerophosphate and 50 µg/mL ascorbic acid and 2) BMP-2 Enriched Media[21,22,25,32]
112 consisting of the OM supplemented with 100 ng/mL BMP-2 (recombinant human BMP-2
113 355-BM-050, R&D Systems). OM provided an environment supportive of osteogenic
114 differentiation due to the addition of β-Glycerophosphate and ascorbic acid, while BMP-2
115 enriched media served as a positive control to drive cells towards the osteoblastic lineage[33].
116 Constructs (n=11) were harvested from each group at days 1, 3, 7, and 15 for analysis of
117 cell proliferation of early and late osteogenic differentiation[34]. These time points were
118 chosen after review of previous literature studying osteogenic differentiation with the
119 C2C12 cell line[25,29,35,36] and specific *in vitro* data showing C2C12 osteogenic
120 differentiation can occur within 48hours in the presence of BMP-2[22,37].

121 At each time point, constructs (n=2) from each group (n=6) were rinsed with PBS,
122 transferred to chamber slides, and incubated with the Live/Dead® Viability/Cytotoxicity
123 Kit (Molecular Probes, Eugene, OR) according to manufacturer's instructions. Specimens
124 were imaged on a fluorescent confocal microscope (Zeiss Axiovert 100 M) to render cross-
125 sectional 2D images and projected 3D images. Live cells are labeled with the green calcein
126 AM fluorophore and dead cells are labeled with the red ethidium homodimer-1
127 fluorophore.

DNA was quantified from constructs (n=3) in each group to estimate cell number and proliferation. Samples were flash frozen in liquid nitrogen, homogenized with a sterilized tissue press, and lysed in 1 mL mammalian protein extraction reagent (M-PER®, ThermoScientific, Waltham, MA). Samples were centrifuged and supernatants collected for analysis using the Quant-iT™ PicoGreen® dsDNA Assay Kit (ThermoScientific).

Cell attachment, morphology, and surface distribution were characterized by electron microscopy. Specimens were removed from dishes in each group at every time point, washed with PBS, fixed in 2.5% glutaraldehyde for 3 hours, and imaged on a Hitachi S-2600 scanning electron microscope (SEM).

For histology, specimens from each group were removed from dishes, fixed in 10% formalin for 48 hours, decalcified with Immunocal® (Decal Chemical Cort, Tallman, NY) for 3-5 days, processed, and embedded in paraffin. Sections were mounted and stained with hematoxylin and eosin (H&E), Masson's trichrome, or 4',6-diamidino-2-phenylindole (DAPI) mounting media (ProLong® Gold Antifade Mountant, ThermoScientific).

The alkaline phosphatase (ALP) enzyme activity was measured from constructs (n=3) using methods previously described.[36,38-42] Each reaction was read in triplicate by loading 150 µL from each tube into 96 well plates and measuring absorbance at 405 nm on a microplate reader (Spectra Max 340 PC). Cell-specific ALP activity was determined by normalizing enzyme activity to the respective sample's DNA content determined by Pico Green assay.[38,43,44]

Immunohistochemistry (IHC) was performed with an anti-Placental ALP (Abcam ab16695, Cambridge, United Kingdom) primary antibody that reacts with cell membrane-bound enzyme followed by a secondary biotin-conjugated anti-rabbit antibody (BioGenex,

Freemont, CA) linked to horseradish peroxidase. Slides were developed with diaminobenzidine substrate (Vector, Burlingame, CA) and counterstained with Meyer's Hematoxylin.

Next, $1x10^6$ MC3T3-E1 cells suspended in 50 µL of alpha-minimum essential medium (α-MEM)+10% FBS were seeded and incubated on the scaffold for 1 hour in 50 µL of α-MEM+10% FBS, before being submerged in 750 µL of α-MEM+10% FBS with 50 µM ascorbic acid and incubated at 37°C for 7 days (n=18). Control monolayers of 1 x 10^4 cells were also incubated at 37°C for 7 days in 250 µL α-MEM+10% FBS with 50 µM ascorbic acid during this time (n=9). The presence of ascorbic acid provides a supportive environment for MC3T3-E1 cell differentiation.[45,46] After 7 days, RNA was isolated from the scaffolds by vigorous agitation in Buffer RLT (RNeasy Mini Kit, QIAGEN, Hilden, Germany) for 30 minutes, and RNA purified following manufacturer instructions. RNA from monolayers was isolated following manufacturer instructions using the RNeasy Mini Kit. cDNA was produced through reverse transcription using High Capacity cDNA Reverse Transcription Kit (Applied Biosystems) and analyzed for gene expression of osteoblast markers using quantitative PCR (ALP and BMP-7). Target gene expression was normalized to the housekeeping gene 18S ribosomal RNA. Relative gene expression was quantified using the $2^{-\Delta\Delta Ct}$ methodology.[47]

In vivo

To demonstrate cell viability and osteoinductivity *in vivo,* scaffolds (n=25) seeded with MC3T3-E1 cells overnight (1 x 10^6 suspended in 50 ul α-MEM+10% FBS) were subcutaneously implanted in 7-week-old male C57BL/6 mice (Jackson Labs) for 4 weeks under a Wake Forest School of Medicine IACUC Protocol #A16-197. Scaffolds without

cells were implanted to serve as a negative control (n=15). A subset of scaffolds (n=12 with cells, n=7 without cells) underwent microcomputed-tomography (microCT) scanning (TriFoil Imaging Triumph PET/CT, voxel size 1 mm) before cell seeding and implantation. Upon explantation, constructs were placed in Buffer RLT (QIAGEN) and vortexed to extract RNA or placed in 10% formalin for repeat microCT scanning to assess new bone formation. RNA was extracted from explanted scaffolds and analyzed for gene markers of osteogenic differentiation (ALP, receptor activator of nuclear factor κ B ligand (RANKL), BMP-2, and BMP-7) using quantitative PCR (n=13 with cells, n=8 without cells). Target gene expression was normalized to the housekeeping gene 18S. Relative gene expression was quantified using the $2^{-\Delta\Delta Ct}$ methodology. Bone formation in the scaffolds by serial microCT scanning was assessed by change in bone volume/total volume ratio (BV/TV) and trabecular thickness (Tb.Th) using MicroView 3D Image Viewer and Analysis Tool (Parallax Innovations, Ilderton, ON, Canada). After microCT scanning, samples were fixed in 10% formalin overnight and subsequently decalcified in 14% neutral, saturated EDTA for 7-14 days. Samples were processed and embedded in paraffin. Sections were stained with Russel-Movat Pentachrome (American MasterTech Scientific Inc; St. Lodi, CA) and IHC was performed using primary antibodies against osteopontin (Abcam ab8448) and ALP (R&D Systems FAB1448A) to identify active bone remodeling, angiogenesis, and new bone formation.

Multiple group comparisons were performed using one-way ANOVA, t-tests were performed on independent means when comparing two groups, and paired t-tests were used when comparing paired groups. Statistical significance was determined when α error < 0.05.

Results

C2C12 pre-osteoblasts proliferated on scaffolds and deposited extracellular matrix (ECM) components. 3D images demonstrated circumferential cell attachment evenly around the pores. Live (green) signal increased during incubation with the strongest signal noted at day 15 (Figure 1). Dead (red) signal was strongest on day 1, likely due to early contact inhibition after seeding constructs at a high cell density. DNA content on DBM was greater than scaffolds at every time point, indicating higher cell density. BMP had no consistent effect on cell proliferation. Cells seeded on the scaffold proliferated as demonstrated by increased DNA at each time point. The differences were significant between day 1 and 15 ($p<0.01$) and day 3 and 15 ($p=0.01$). Similarly, DNA content on DBM increased at each time point as well (Figure 2). DAPI and H&E sections (Figure 3) confirmed higher cell density on DBM relative to scaffolds. SEM supported this finding with denser cell distribution on DBM samples relative to scaffolds at day 7 and 15 (Figure 4). ECM was deposited uniformly at later time points, and BMP-2 did not change cell morphology, density, or distribution on matrices. Molecular assays showed that cells seeded on scaffolds had greater ALP enzyme activity at days 7 and 15 ($p<0.0001$) compared to cells seeded on DBM or gelfoam constructs (Figure 5). BMP-2 increased ALP activity on all constructs; this increase was significant only for scaffolds (days 3 ($p=0.005$), 7 ($p=0.02$), 15 ($p<0.0001$)) suggestive of an additive effect on this matrix. ALP IHC staining increased at day 15 and supported the above cell-specific enzyme activity findings (Figure 6). MC3T3-E1 cells pre-seeded on scaffolds demonstrated greater ALP expression than cell monolayers ($p=0.0021$); however, BMP-7 expression was similar (data not

shown). These results indicate the scaffold construct may possess osteoinductive potential *in vitro*.

In vivo expression of ALP, BMP-7, and BMP-2 increased within the pre-seeded scaffolds; however, only ALP was significant (p=0.0009) (Figure 7). RANKL gene expression was equal between groups. MicroCT analysis was performed on 9 seeded and 4 un-seeded scaffolds. These data demonstrated greater changes in BV/TV and Tb.Th in the pre-seeded scaffolds; however, only Tb.Th reached significance (p=0.03). Paired t-tests showed significantly increased BV/TV (p=0.0013) and Tb.Th (p=0.0002) after explantation in both groups (n=13) indicating new bone formation, regardless of cell seeding (Figure 8). Pentachrome staining demonstrated angiogenesis and new bone formation within the scaffold (Figure 9). IHC analysis revealed positive staining for OPN and ALP. These results proved that the scaffold maintains osteoinductive properties following decellularization, due to its ability to recruit and stimulate cells down a bone forming lineage *in vivo*.

Discussion

Large bone defects resulting from trauma, infection, or tumor resection often require bone grafting to fill the defect[1,7]. The gold standard for bone grafting is autologous bone graft; however, limited quantity and structural deficiencies preclude its use in larger defects. Allograft is a suitable alternative, but this has been associated with the transmission of infectious diseases[7,8]. Additionally, the quantity of donor bone is limited, and donor biology cannot be controlled, resulting in considerable variability in graft quality[8]. Therefore, tissue engineering plays an increased role in developing alternatives[48,49]. One possibility is the use of xenografts. Our laboratory established a

novel decellularization and oxidation technique using peracetic acid that removes 98% of DNA when applied to porcine bone[20]. Our current study demonstrates that this treatment protocol preserves at least some of the native porcine bone's osteoinductive potential in the decellularized scaffold. *In vitro* results were comparable to demineralized bone matrix, a commercial product currently in clinical use with proven osteoinductive potential.

There are limitations to our study. First, clinical translation of *in vitro* and animal experiments is limited. However, we believe these experiments were a necessary first step to determine the properties of this bone scaffold after undergoing the decellularization and oxidation procedure. Second, our *in vivo* experiments involve an ectopic subcutaneous implantation model, rather than an orthotopic bone void filling model. However, the purpose of these experiments was solely to determine the osteoinductive potential of this scaffold in an *in vivo* environment. Additionally, RNA collection may have been limited due to the porous nature of the scaffold. However, we attempted to minimize this by vigorous agitation of the scaffold for 30 minutes. Finally, a major limitation is the use of murine rather than human cell lines for these experiments, which limits immediate clinical translation. These cell lines, however, have been validated for study of biomaterials osteoinductive potential previously[50,51]. The use of murine cells also permitted the analysis of immune reactivity and scaffold rejection, which did not occur in our study.

BMP-2 is one of the strongest stimulants of osteogenic differentiation in the pre-osteoblast cell lines used in our experiments[22,23,37,51-53]. Concentrations as low as 100 ng/mL and 50 ng/mL were sufficient to promote osteogenic differentiation with increased

ALP activity in MC3T3-E1[53] and C2C12[22], respectively. However, few reports studied osteogenic differentiation of cells seeded onto xenograft derived bone scaffolds[38,40,43,44,54]. Hashimoto et al.[43] demonstrated that porcine hydroxyapatite contains osteoinductive properties and that these properties are maintained after processing[43]. Similarly, Smith et al.[55] found that the osteoinductive properties were maintained in allografts following a decellularization and washing procedure. However, Bormann et al.[37] used a similar decellularization and oxidation protocol to ours with the addition of peracetic acid on allograft specimens and found that the osteoinductive potential was not maintained. In the present study, we applied a novel decellularization and oxidation technique using peracetic acid that removed 98% of the porcine DNA from the bone scaffolds[20]. Contrary to the findings by Boorman et al.[37], our results demonstrate that the xenograft does indeed maintain osteoinductive potential after processing. C2C12 and MC3T3-E1 cells attached to the scaffold matrix, proliferated, and underwent osteogenic differentiation during the incubation period. The discrepancy between these studies outlines the variability between decellularization techniques as well as allograft specimens. Bormann et al.[37] reported that the donors for the samples used ranged in age from 13-67 years old, and gender could be a source of variability between samples. These discrepancies may affect osteoinductive capacity[56] and outline the importance of controlling environmental factors that may influence the quality of the donor bone, which is only possible with the use of a xenograft.

In vivo assessment of the porcine bone scaffold demonstrated spontaneous new bone formation and angiogenesis. The identification of angiogenesis represents a critical finding due to the lack of vascularization being one of the major limitations associated

with the use of tissue engineered constructs during early bone regeneration[57,58]. The presence of angiogenesis signifies graft-host integration by the induction of inflammatory cytokines as part of the normal healing process[59]. It is reasonable to conclude that the presence of angiogenesis allowed for new bone formation due to the known importance angiogenesis has in bone repair and regeneration[59]. Accordingly, Hirata et al.[60] found that a BMP-2 soaked absorbable collagen sponge implanted in humans led to new bone formation lined by endothelial cells. Furthermore, Bhumiratana et al.[61] implanted a clinically approved decellularized bovine trabecular bone seeded with adipose-derived stem cells into Yucatan minipig skull defects and concluded that angiogenesis and new bone formation occurred in parallel.

Overall, our data demonstrate that a novel decellularization and oxidation technique applied to porcine metaphyseal bone preserves the osteoinductive nature of the bone. Previous literature identifies that these properties are the most difficult to artificially create in synthetic scaffolds and to maintain when processing bone scaffolds, therefore outlining the potential clinical impact of this construct. Future studies involving this xenograft will focus on placing the construct within a bone defect, identifying osseointegration, and comparing it to current standard treatments. These experiments will look at the effect of supplementing the scaffold with human mesenchymal stem cells, as a step towards clinical translation. Furthermore, an *in vivo* analysis of inflammatory markers to confirm that the bone scaffold has no increased reactivity when compared to currently used clinical implants for large bone defects should be performed.

Acknowledgments

We thank the Orthopaedic Research and Education Foundation (OREF) and AO Trauma North America for their contribution to the funding of this project through a Resident Clinician Scientist Research Grant. We would also like to thank the Musculoskeletal Transplant Foundation (MTF) for their donation of human DBM samples at no cost. The animal experiments were supported by a CTSI Ignition Fund under the NIH/NCATS UL1 TR001420 grant. We would like to thank Ms. Eileen Elsner, Ms. Jiaozhong Cia, and Dr. Lihong Shi for their help with tissue processing and animal handling throughout these experiments.

References

1. Calori GM, Mazza E, Colombo M, Ripamonti C. The use of bone-graft substitutes in large bone defects: any specific needs? *Injury.* Sep 2011;42 Suppl 2:S56-63.
2. Fassbender M, Minkwitz S, Thiele M, Wildemann B. Efficacy of two different demineralised bone matrix grafts to promote bone healing in a critical-size-defect: a radiological, histological and histomorphometric study in rat femurs. *International orthopaedics.* Sep 2014;38(9):1963-1969.
3. Kolambkar YM, Dupont KM, Boerckel JD, et al. An alginate-based hybrid system for growth factor delivery in the functional repair of large bone defects. *Biomaterials.* Jan 2011;32(1):65-74.
4. Roddy E, DeBaun MR, Daoud-Gray A, Yang YP, Gardner MJ. Treatment of critical-sized bone defects: clinical and tissue engineering perspectives. *European journal of orthopaedic surgery & traumatology : orthopedie traumatologie.* Apr 2018;28(3):351-362.
5. Khan SN, Cammisa FP, Jr., Sandhu HS, Diwan AD, Girardi FP, Lane JM. The biology of bone grafting. *The Journal of the American Academy of Orthopaedic Surgeons.* Jan-Feb 2005;13(1):77-86.
6. Albrektsson T, Johansson C. Osteoinduction, osteoconduction and osseointegration. *Eur Spine J.* Oct 2001;10 Suppl 2:S96-101.
7. Campana V, Milano G, Pagano E, et al. Bone substitutes in orthopaedic surgery: from basic science to clinical practice. *J Mater Sci Mater Med.* Oct 2014;25(10):2445-2461.
8. De Long WG, Jr., Einhorn TA, Koval K, et al. Bone grafts and bone graft substitutes in orthopaedic trauma surgery. A critical analysis. *The Journal of bone and joint surgery. American volume.* Mar 2007;89(3):649-658.
9. Zimmermann G, Moghaddam A. Allograft bone matrix versus synthetic bone graft substitutes. *Injury.* Sep 2011;42 Suppl 2:S16-21.
10. Fielding G, Bose S. SiO2 and ZnO dopants in three-dimensionally printed tricalcium phosphate bone tissue engineering scaffolds enhance osteogenesis and angiogenesis in vivo. *Acta biomaterialia.* Nov 2013;9(11):9137-9148.
11. Hsu EL, Ghodasra JH, Ashtekar A, et al. A comparative evaluation of factors influencing osteoinductivity among scaffolds designed for bone regeneration. *Tissue engineering. Part A.* Aug 2013;19(15-16):1764-1772.
12. Pierson RN, 3rd, Dorling A, Ayares D, et al. Current status of xenotransplantation and prospects for clinical application. *Xenotransplantation.* Sep-Oct 2009;16(5):263-280.
13. Wancket LM. Animal Models for Evaluation of Bone Implants and Devices: Comparative Bone Structure and Common Model Uses. *Vet Pathol.* Sep 2015;52(5):842-850.
14. Cooper DKC, Ekser B, Tector AJ. Immunobiological barriers to xenotransplantation. *International journal of surgery.* Nov 2015;23(Pt B):211-216.
15. Vadori M, Cozzi E. The immunological barriers to xenotransplantation. *Tissue antigens.* Oct 2015;86(4):239-253.
16. Whitlock PW, Seyler TM, Parks GD, et al. A novel process for optimizing musculoskeletal allograft tissue to improve safety, ultrastructural properties, and cell infiltration. *The Journal of bone and joint surgery. American volume.* Aug 15 2012;94(16):1458-1467.

17. Whitlock PW, Smith TL, Poehling GG, Shilt JS, Van Dyke M. A naturally derived, cytocompatible, and architecturally optimized scaffold for tendon and ligament regeneration. *Biomaterials.* Oct 2007;28(29):4321-4329.
18. Seyler TM, Bracey DN, Plate JF, et al. The Development of a Xenograft-Derived Scaffold for Tendon and Ligament Reconstruction Using a Decellularization and Oxidation Protocol. *Arthroscopy : the journal of arthroscopic & related surgery : official publication of the Arthroscopy Association of North America and the International Arthroscopy Association.* Feb 2017;33(2):374-386.
19. Bracey DN, Seyler TM, Jinnah AH, et al. A Decellularized Porcine Xenograft-Derived Bone Scaffold for Clinical Use as a Bone Graft Substitute: A Critical Evaluation of Processing and Structure. *Journal of functional biomaterials.* Jul 12 2018;9(3).
20. Bracey DN. *A Decellularized Porcine Xenograft-Derived Bone Scaffold for Clinical Use as a Bone Graft Substitute: A Critical Evaluation of Processing and Structure*: Orthopaedic Surgery, Wake Forest University Graduate School of Arts & Sciences; 2017.
21. Ansari S, Moshaverinia A, Pi SH, Han A, Abdelhamid AI, Zadeh HH. Functionalization of scaffolds with chimeric anti-BMP-2 monoclonal antibodies for osseous regeneration. *Biomaterials.* Dec 2013;34(38):10191-10198.
22. Han B, Tang B, Nimni ME. Quantitative and sensitive in vitro assay for osteoinductive activity of demineralized bone matrix. *Journal of orthopaedic research : official publication of the Orthopaedic Research Society.* Jul 2003;21(4):648-654.
23. Katagiri T, Yamaguchi A, Komaki M, et al. Bone morphogenetic protein-2 converts the differentiation pathway of C2C12 myoblasts into the osteoblast lineage. *J Cell Biol.* Dec 1994;127(6 Pt 1):1755-1766.
24. Shi Q, Li Y, Sun J, et al. The osteogenesis of bacterial cellulose scaffold loaded with bone morphogenetic protein-2. *Biomaterials.* Oct 2012;33(28):6644-6649.
25. Yang Q, Jian J, Abramson SB, Huang X. Inhibitory effects of iron on bone morphogenetic protein 2-induced osteoblastogenesis. *J Bone Miner Res.* Jun 2011;26(6):1188-1196.
26. Araujo-Gomes N, Romero-Gavilan F, Garcia-Arnaez I, et al. Osseointegration mechanisms: a proteomic approach. *Journal of biological inorganic chemistry : JBIC : a publication of the Society of Biological Inorganic Chemistry.* Mar 23 2018.
27. Shuang Y, Yizhen L, Zhang Y, Fujioka-Kobayashi M, Sculean A, Miron RJ. In vitro characterization of an osteoinductive biphasic calcium phosphate in combination with recombinant BMP2. *BMC oral health.* Aug 2 2016;17(1):35.
28. Hupkes M, Sotoca AM, Hendriks JM, van Zoelen EJ, Dechering KJ. MicroRNA miR-378 promotes BMP2-induced osteogenic differentiation of mesenchymal progenitor cells. *BMC Mol Biol.* 2014;15(1):1.
29. Shui W, Zhang W, Yin L, et al. Characterization of scaffold carriers for BMP9-transduced osteoblastic progenitor cells in bone regeneration. *J Biomed Mater Res A.* Oct 16 2013.
30. Sondag GR, Salihoglu S, Lababidi SL, et al. Osteoactivin Induces Transdifferentiation of C2C12 Myoblasts into Osteoblasts. *J Cell Physiol.* Nov 22 2013.
31. Yu S, Geng Q, Ma J, et al. Heparin-binding EGF-like growth factor and miR-1192 exert opposite effect on Runx2-induced osteogenic differentiation. *Cell Death Dis.* 2013;4:e868.

32. Feichtinger GA, Morton TJ, Zimmermann A, et al. Enhanced reporter gene assay for the detection of osteogenic differentiation. *Tissue engineering. Part C, Methods.* Apr 2011;17(4):401-410.
33. Langenbach F, Handschel J. Effects of dexamethasone, ascorbic acid and beta-glycerophosphate on the osteogenic differentiation of stem cells in vitro. *Stem cell research & therapy.* 2013;4(5):117.
34. Coelho MJ, Fernandes MH. Human bone cell cultures in biocompatibility testing. Part II: effect of ascorbic acid, beta-glycerophosphate and dexamethasone on osteoblastic differentiation. *Biomaterials.* Jun 2000;21(11):1095-1102.
35. Rivera JC, Strohbach CA, Wenke JC, Rathbone CR. Beyond osteogenesis: an in vitro comparison of the potentials of six bone morphogenetic proteins. *Frontiers in pharmacology.* 2013;4:125.
36. Shi K, Lu J, Zhao Y, et al. MicroRNA-214 suppresses osteogenic differentiation of C2C12 myoblast cells by targeting Osterix. *Bone.* Aug 2013;55(2):487-494.
37. Bormann N, Pruss A, Schmidmaier G, Wildemann B. In vitro testing of the osteoinductive potential of different bony allograft preparations. *Archives of orthopaedic and trauma surgery.* Jan 2010;130(1):143-149.
38. Arca T, Proffitt J, Genever P. Generating 3D tissue constructs with mesenchymal stem cells and a cancellous bone graft for orthopaedic applications. *Biomed Mater.* Apr 2011;6(2):025006.
39. Liu G, Sun J, Li Y, et al. Evaluation of partially demineralized osteoporotic cancellous bone matrix combined with human bone marrow stromal cells for tissue engineering: an in vitro and in vivo study. *Calcified tissue international.* Sep 2008;83(3):176-185.
40. Marcos-Campos I, Marolt D, Petridis P, Bhumiratana S, Schmidt D, Vunjak-Novakovic G. Bone scaffold architecture modulates the development of mineralized bone matrix by human embryonic stem cells. *Biomaterials.* Nov 2012;33(33):8329-8342.
41. Stiehler M, Seib FP, Rauh J, et al. Cancellous bone allograft seeded with human mesenchymal stromal cells: a potential good manufacturing practice-grade tool for the regeneration of bone defects. *Cytotherapy.* Sep 2010;12(5):658-668.
42. Thibault RA, Scott Baggett L, Mikos AG, Kasper FK. Osteogenic differentiation of mesenchymal stem cells on pregenerated extracellular matrix scaffolds in the absence of osteogenic cell culture supplements. *Tissue engineering. Part A.* Feb 2010;16(2):431-440.
43. Hashimoto Y, Funamoto S, Kimura T, Nam K, Fujisato T, Kishida A. The effect of decellularized bone/bone marrow produced by high-hydrostatic pressurization on the osteogenic differentiation of mesenchymal stem cells. *Biomaterials.* Oct 2011;32(29):7060-7067.
44. Kouroupis D, Baboolal TG, Jones E, Giannoudis PV. Native multipotential stromal cell colonization and graft expander potential of a bovine natural bone scaffold. *Journal of orthopaedic research : official publication of the Orthopaedic Research Society.* Jul 19 2013.
45. Torii Y, Hitomi K, Tsukagoshi N. L-ascorbic acid 2-phosphate promotes osteoblastic differentiation of MC3T3-E1 mediated by accumulation of type I collagen. *Journal of nutritional science and vitaminology.* Jun 1994;40(3):229-238.
46. Franceschi RT, Iyer BS, Cui Y. Effects of ascorbic acid on collagen matrix formation and osteoblast differentiation in murine MC3T3-E1 cells. *Journal of bone and mineral*

research : the official journal of the American Society for Bone and Mineral Research. Jun 1994;9(6):843-854.

47. Livak KJ, Schmittgen TD. Analysis of relative gene expression data using real-time quantitative PCR and the 2(-Delta Delta C(T)) Method. *Methods (San Diego, Calif.)*. Dec 2001;25(4):402-408.
48. Frohlich M, Grayson WL, Wan LQ, Marolt D, Drobnic M, Vunjak-Novakovic G. Tissue engineered bone grafts: biological requirements, tissue culture and clinical relevance. *Current stem cell research & therapy.* Dec 2008;3(4):254-264.
49. Liu Y, Chan JK, Teoh SH. Review of vascularised bone tissue-engineering strategies with a focus on co-culture systems. *Journal of tissue engineering and regenerative medicine.* Feb 2015;9(2):85-105.
50. Kanayama S, Kaito T, Kitaguchi K, et al. ONO-1301 Enhances in vitro Osteoblast Differentiation and in vivo Bone Formation Induced by Bone Morphogenetic Protein. *Spine.* Oct 9 2017.
51. Qadir AS, Um S, Lee H, et al. miR-124 negatively regulates osteogenic differentiation and in vivo bone formation of mesenchymal stem cells. *J Cell Biochem.* May 2015;116(5):730-742.
52. Heo SY, Ko SC, Nam SY, et al. Fish bone peptide promotes osteogenic differentiation of MC3T3-E1 pre-osteoblasts through upregulation of MAPKs and Smad pathways activated BMP-2 receptor. *Cell biochemistry and function.* Apr 2018;36(3):137-146.
53. Fu C, Yang X, Tan S, Song L. Enhancing Cell Proliferation and Osteogenic Differentiation of MC3T3-E1 Pre-osteoblasts by BMP-2 Delivery in Graphene Oxide-Incorporated PLGA/HA Biodegradable Microcarriers. *Scientific reports.* Oct 2 2017;7(1):12549.
54. Lu X, Wang J, Li B, Zhang Z, Zhao L. Gene expression profile study on osteoinductive effect of natural hydroxyapatite. *J Biomed Mater Res A*. Sep 25 2013.
55. Smith CA, Richardson SM, Eagle MJ, Rooney P, Board T, Hoyland JA. The use of a novel bone allograft wash process to generate a biocompatible, mechanically stable and osteoinductive biological scaffold for use in bone tissue engineering. *Journal of tissue engineering and regenerative medicine.* May 2015;9(5):595-604.
56. Smith CA, Board TN, Rooney P, Eagle MJ, Richardson SM, Hoyland JA. Human decellularized bone scaffolds from aged donors show improved osteoinductive capacity compared to young donor bone. *PloS one.* 2017;12(5):e0177416.
57. Giannoni P, Scaglione S, Daga A, Ilengo C, Cilli M, Quarto R. Short-time survival and engraftment of bone marrow stromal cells in an ectopic model of bone regeneration. *Tissue engineering. Part A.* Feb 2010;16(2):489-499.
58. Muschler GF, Nakamoto C, Griffith LG. Engineering principles of clinical cell-based tissue engineering. *The Journal of bone and joint surgery. American volume.* Jul 2004;86-A(7):1541-1558.
59. Stegen S, van Gastel N, Carmeliet G. Bringing new life to damaged bone: the importance of angiogenesis in bone repair and regeneration. *Bone.* Jan 2015;70:19-27.
60. Hirata A, Ueno T, Moy PK. Newly Formed Bone Induced by Recombinant Human Bone Morphogenetic Protein-2: A Histological Observation. *Implant dentistry.* Apr 2017;26(2):173-177.
61. Bhumiratana S, Bernhard JC, Alfi DM, et al. Tissue-engineered autologous grafts for facial bone reconstruction. *Science translational medicine.* Jun 15 2016;8(343):343ra383.

Legends

Figure 1. Live/Dead Stained Confocal Microscopy Images
Demineralized Bone Matrix (DBM), scaffold, and gelfoam matrices were seeded with 1 million C2C12 pre-osteoblast cells and incubated to select time points. Cross sectional images were captured at 10x magnification and overlayed to create the shown 3d projections. On day 1, matrices were switched into osteogenic media (OM) enriched with 100 ng/ml BMP-2. Representative micrographs show green fluorophore (calcein AM) staining of live cells and red fluorophore (ethidium) staining of dead cells. Constructs had notable autofluorescence with ethidium staining as shown in the "blank" images. Cell density increased with time on all 3 matrices, consistent with DNA quantification results.

Figure 2. DNA Content in Seeded Constructs
Constructs were harvested at select time points, and DNA content was measured with the PicoGreen® assay.
*<0.05, **<0.01, ***<0.001

(a) scaffold vs DBM; **(b)** scaffold vs GF; **(c)** DBM vs GF
(d) scaffold OM vs BMP; **(e)** DBM OM vs BMP; **(f)** GF OM vs BMP;
(g) DBM day 1 vs 3; **(h)** scaffold day 1 vs 3; **(i)** GF day 1 vs 3;
(j) DBM day 3 vs 7; **(k)** scaffold day 3 vs 7; **(l)** GF day 3 vs 7
(m) DBM day 7 vs 15; **(n)** scaffold day 7 vs 15; **(o)** GF day 7 vs 15
(p) scaffold day 3 vs 15; **(q)** DBM day 3 vs 15; **(r)** GF day 3 vs 15

Figure 3. Cell Density Staining on Different Constructs
DAPI (A and B) and H&E (C and D) stained sections demonstrating higher cell density on DBM (A and C) relative to scaffolds (B and D).

Figure 4. Scanning Electron Microscopy of Cell Density
Scanning electron microscopy images demonstrating a denser cell distribution on DBM samples when compared with scaffolds at days 7 and 15.

Figure 5. Alkaline Phosphatase Enzyme Activity
ALP activity is greater within the cell-seeded scaffolds in osteogenic media (A). ALP activity was significantly greater on scaffolds in a BMP-2 enriched media (B), suggesting an additive effect of the matrix.

Figure 6. **Alkaline Phosphatase Immunohistochemistry**
ALP immunohistochemical staining increased at day 15 in both constructs, confirming that there is increased alkaline phosphatase activity that is similar between constructs.

Figure 7. Gene Expression of Osteogenic Factors
Gene expression of ALP (A; Alk Phos), bone morphogenetic protein (BMP) – 2 (B), and BMP-7 (C) is increased in scaffolds pre-seeded with cells when compared to scaffolds with no cells. However, only alkaline phosphatase reached significance.

Figure 8. MicroCT Analysis of *in vivo* Constructs
Bone volume ratio and trabecular thickness both increase between pre-implantation and explantation ($p=0.0013$ and $p=0.0002$, respectively) signifying new bone formation within the xenograft.

Figure 9. Histological Staining of *in vivo* Constructs
Pentachrome staining demonstrating new vessel formation (black arrow) and new bone formation (blue arrow).

Figure 1

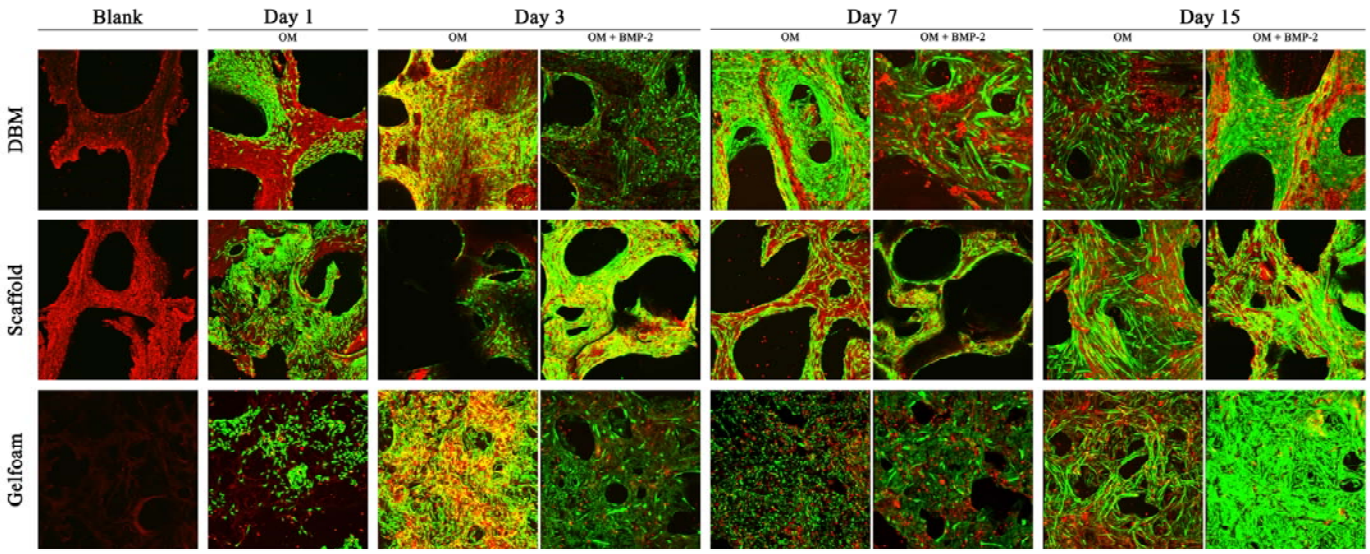

Figure 2

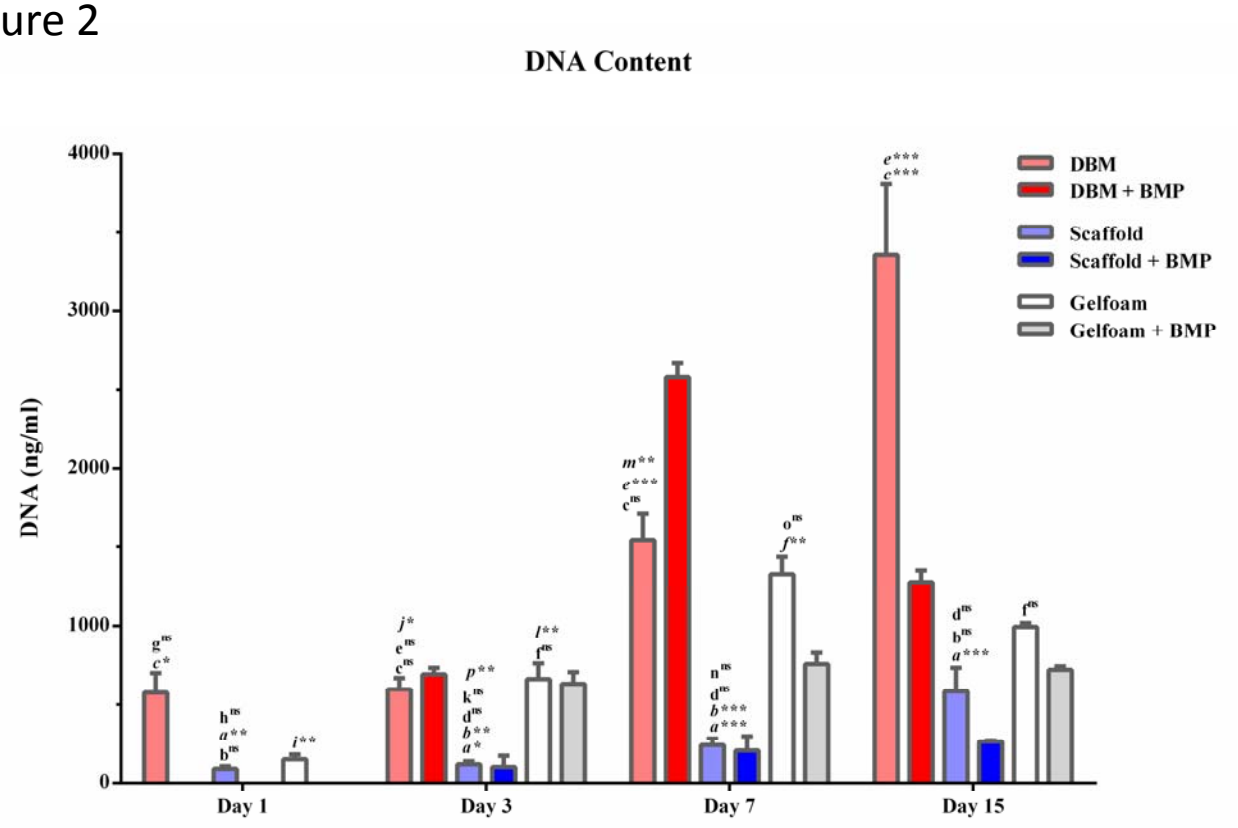

Figure 3

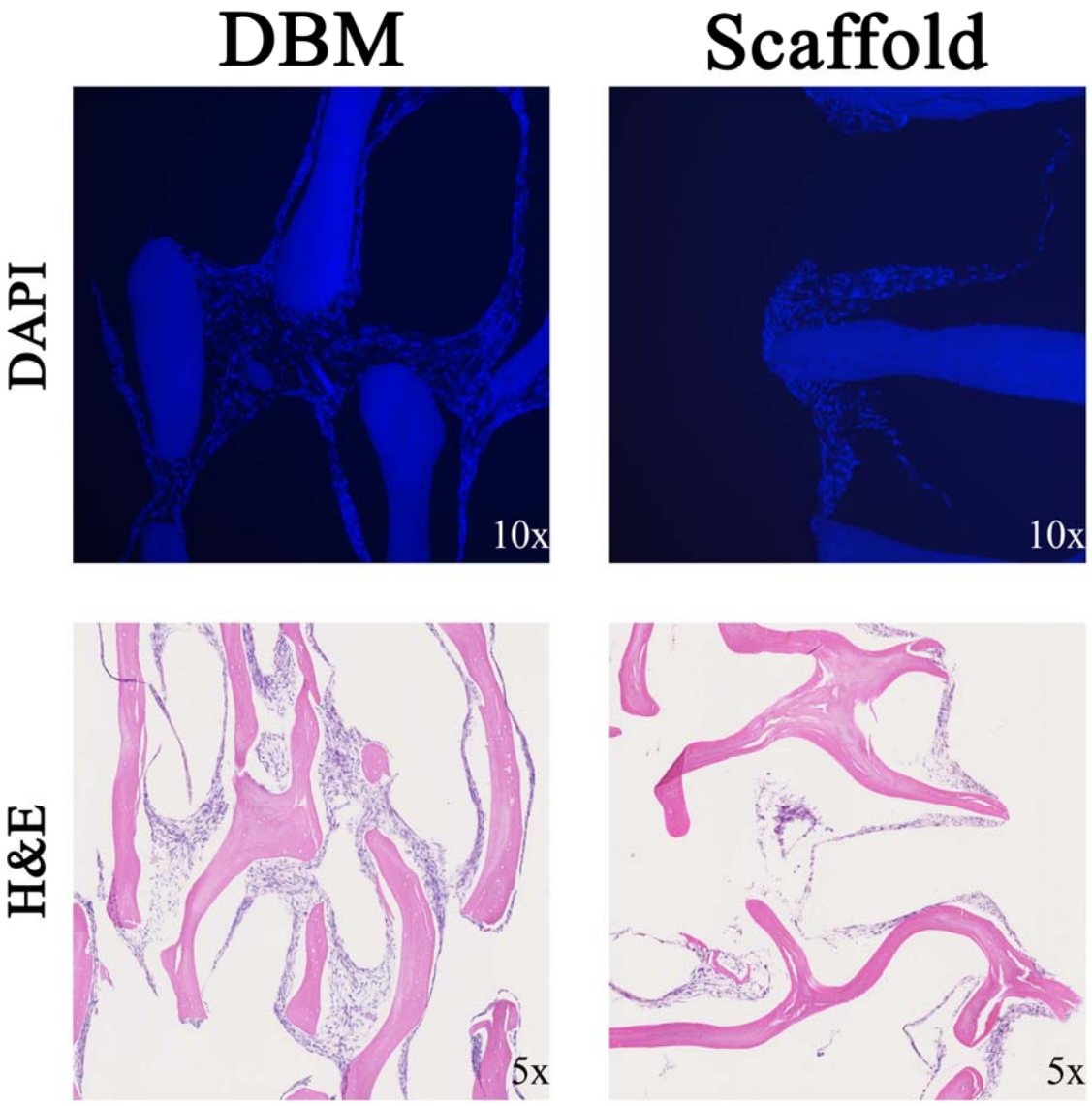

Figure 4

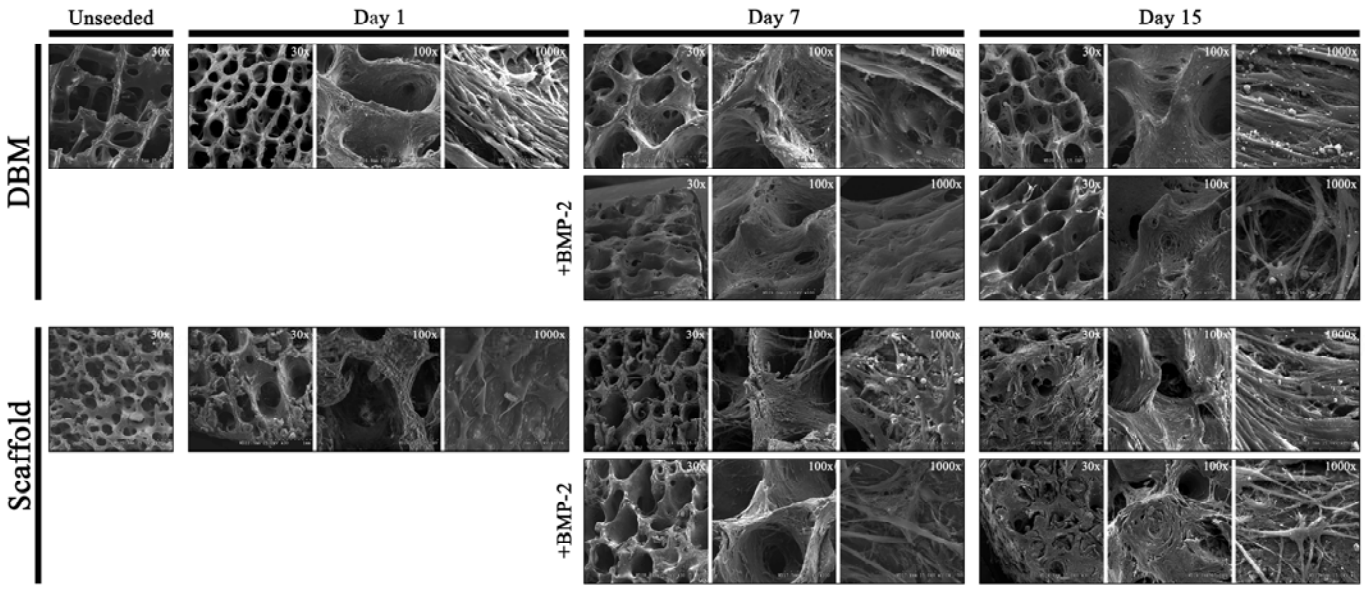

Figure 5

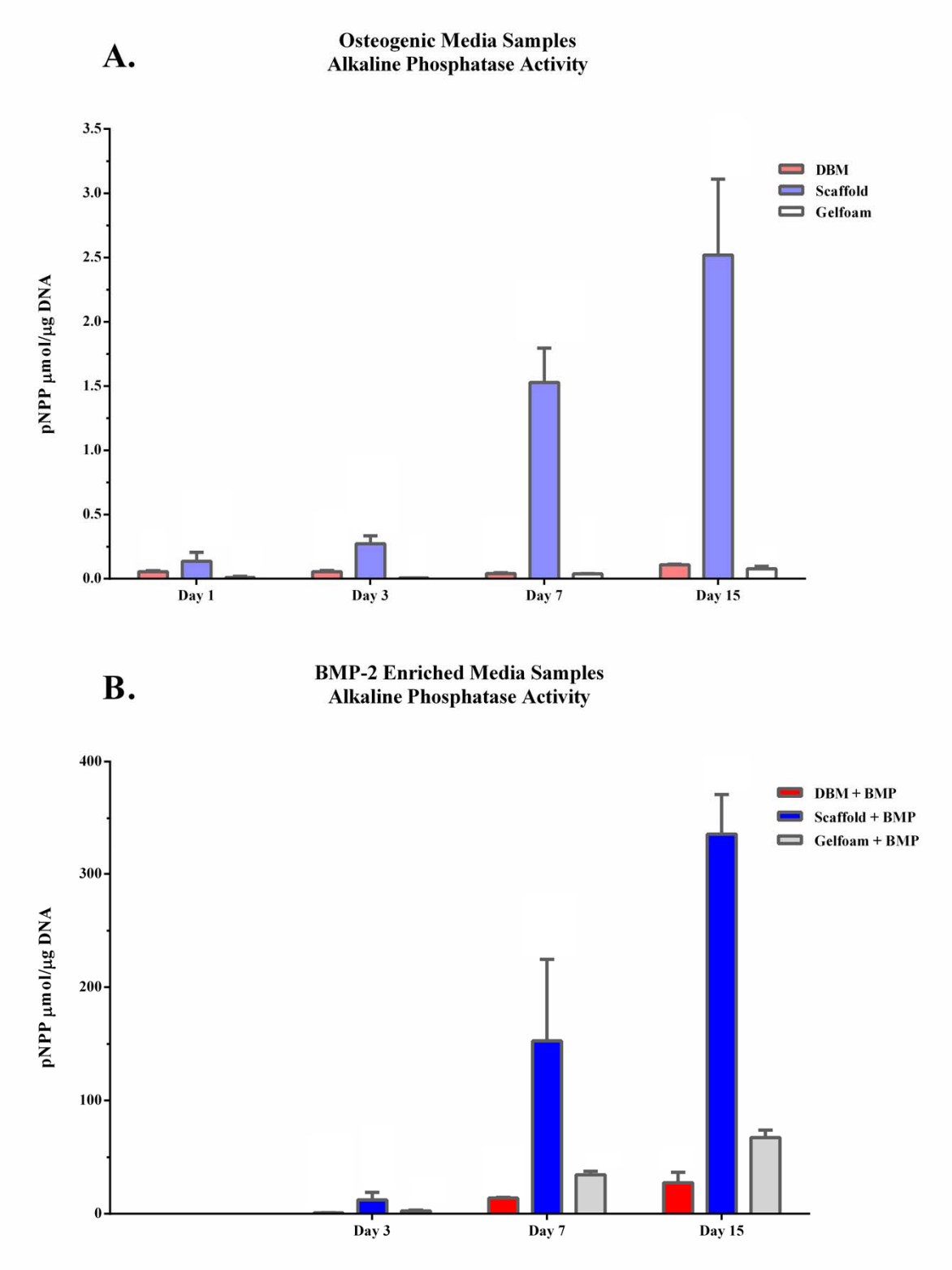

Figure 6

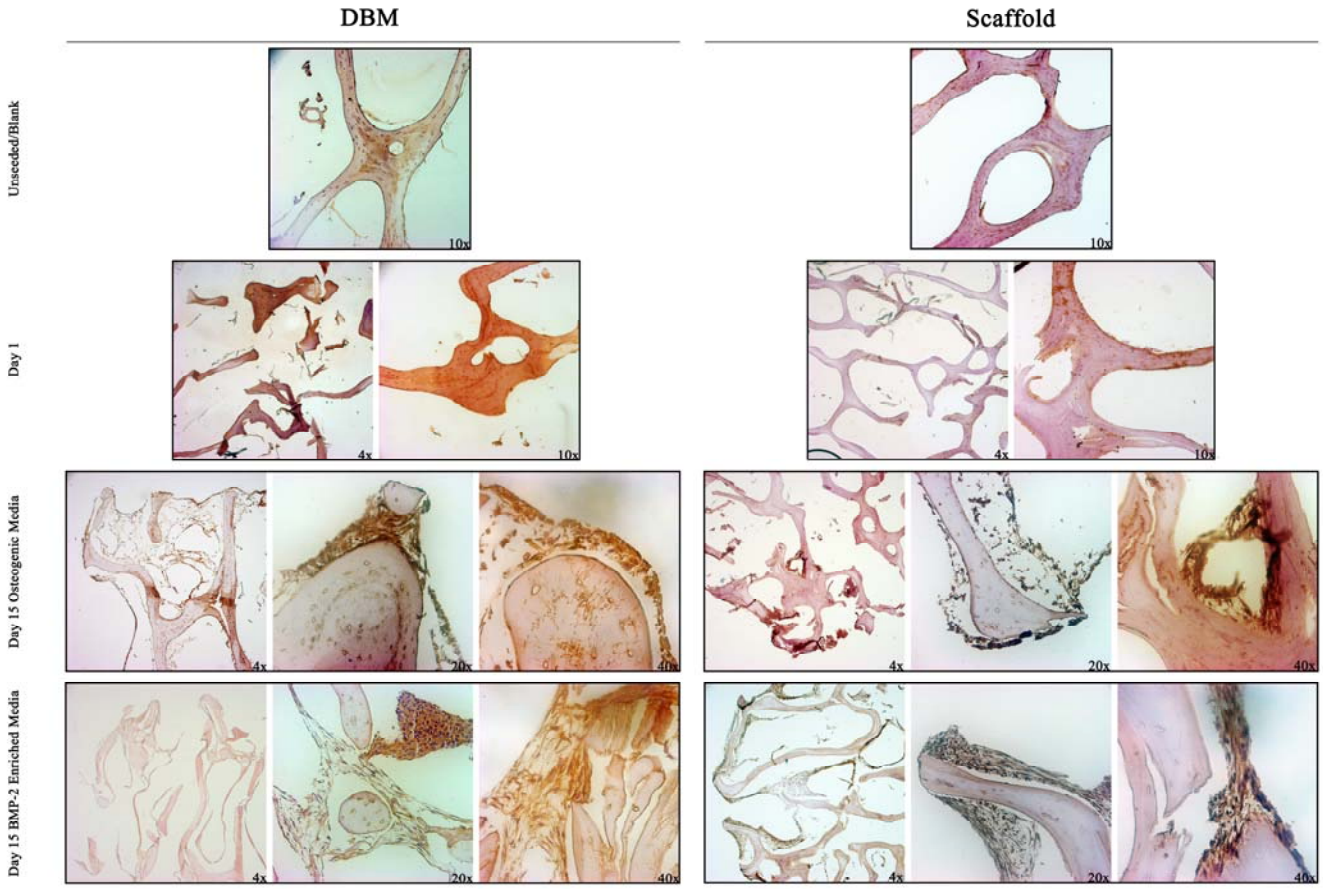

Figure 7

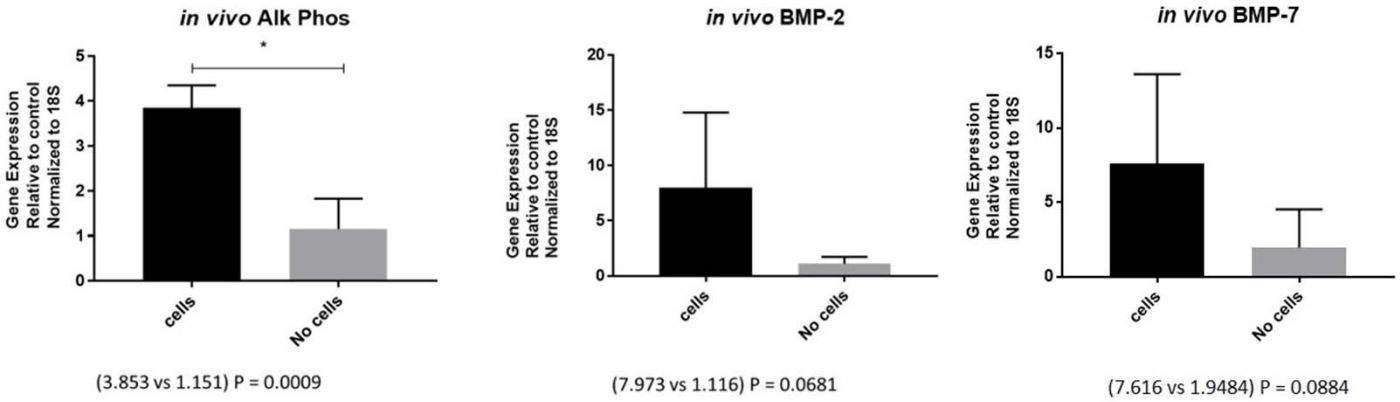

(3.853 vs 1.151) P = 0.0009

(7.973 vs 1.116) P = 0.0681

(7.616 vs 1.9484) P = 0.0884

Figure 8

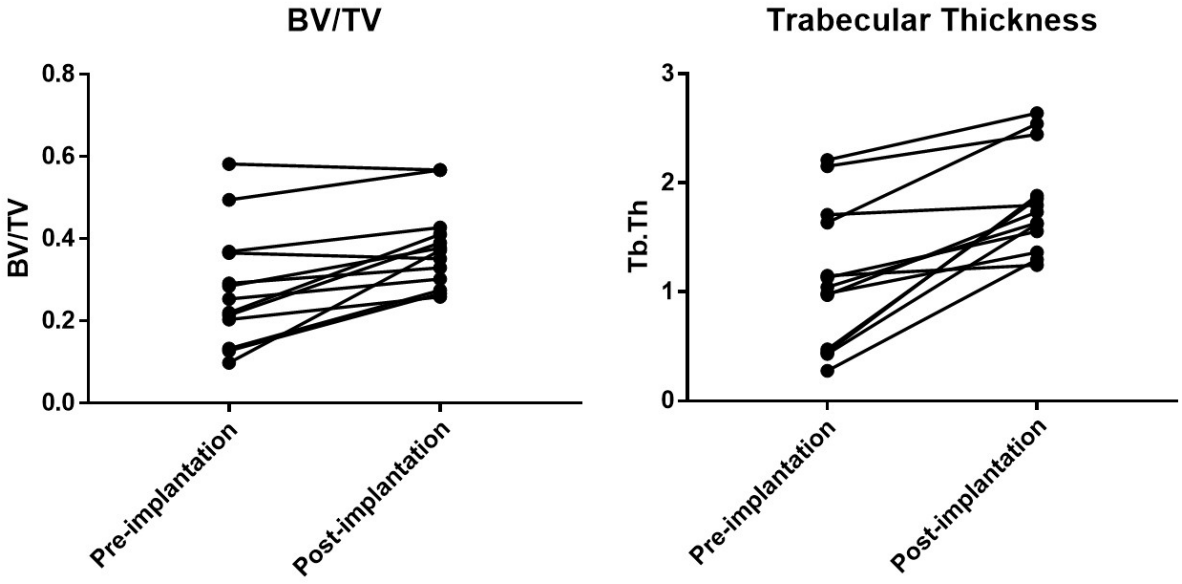

Figure 9